Constraining Pulsar Emission Physics through Radio/Gamma-Ray Correlation of Crab Giant Pulses

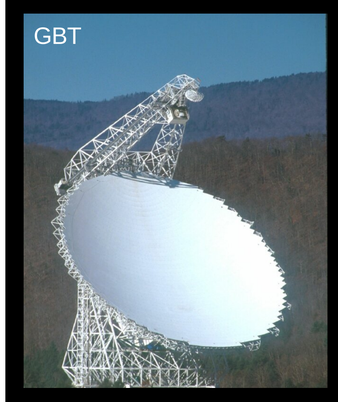

A. V. Bilous (UVa), V. I. Kondratiev (ASTRON), M. A. McLaughlin (WVU),
S. M. Ransom (NRAO), M. Lyutikov (Purdue), M. Mickaliger (WVU), B. Stappers (U. of Manchester),
G. Langston (NRAO), D. R. Lorimer (WVU)

Abstract Summary: The correlation between radio and gamma-emission of Crab pulsar during giant pulses is studied with the goal of constraining the giant-pulse emission mechanism.

Crab Pulsar Radio/Fermi Campaign

To constrain the giant pulse (GP) emission mechanism and test the model of Lyutikov (2007) of GP emission, we are carrying out a campaign of simultaneous observations of the Crab pulsar between γ-rays (Fermi) and radio wavelengths. The correlation between times of arrival of radio GPs and high-energy photons, whether it exists or not, will allow us to choose between different origins of GP emission and further constrain the emission physics. Our foremost goal was testing whether radio GPs are due to changes in the coherence of the radio emission mechanism, variations in the pair creation rate in the pulsar magnetosphere, or changes in the beaming direction. Accomplishing this goal requires an enormous number of simultaneous radio GPs and γ-photons. Thus, we organized a radio observations campaign using the 42-ft telescope at the Jodrell Bank Observatory (UK), the 140-ft telescope, and the 100-m Richard C. Byrd Green Bank Telescope (GBT) at the Green Bank Observatory (WV). While the observations with the two first ones are ongoing, here we present the preliminary results of 20 hrs of observations with the GBT at the high frequency of 8.9 GHz. These particular observations were aimed to probe the model of GP emission by Lyutikov (2007) which predicts that GPs at frequencies > 4 GHz should be accompanied by γ-ray photons of energies of 1-100 GeV.

140-ft, Green Bank

42-ft, Jodrell Bank

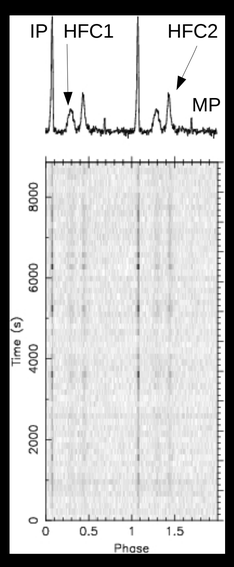

Figure 1. Average Crab radio profile for the GBT session on Sep 25, 2009.

GBT Observations were carried out on Sep 9-28, 2009 at a frequency of 8.9 GHz using the new Green Bank Ultimate Pulsar Processor (GUPPI). The total bandwidth of 800 MHz was split into 256 frequency channels, and the total intensity was recorded with the sampling interval 2.56-3.84 μs. There were 10 observing sessions for a total of ~20 h. The column 2 in the Table lists the duration of simultaneous observations together with Fermi, and the column 3 gives the number of GPs detected stronger than a threshold of 7σ during contemporaneous time with Fermi. Taking into account the contribution from the Crab nebula, the 1σ sensitivity in our observations was about 480 mJy. In total, we found more than 85,000 GPs stronger than 7σ, with about simultaneous 39,450 GPs with Fermi.

The raw data from every session were dedispersed with the current DM of the Crab Pulsar using the PRESTO package, and searched for all the single-pulse events. The lists of events were presented in TEMPO format and converted to barycentric reference frame for further analysis with Fermi data. Figure 1 shows the average profile (top) of the Crab Pulsar together with the subintegrations during the course of observations for the most fruitful session on Sep 25. The interpulse (IP) and high-frequency components (HFCs) are clearly seen. The weak peak after HFC2 represents the main pulse (MP). The comparison with Figure 2 certainly indicates that the majority of the events occur at the phases of MP (stronger) and IP (more frequently). Though several events were detected at the phases of HFCs and even MP precursor (also reported by Jessner et al., 2005), their GP nature is to be checked, and they could only represent strong single pulses of regular emission.

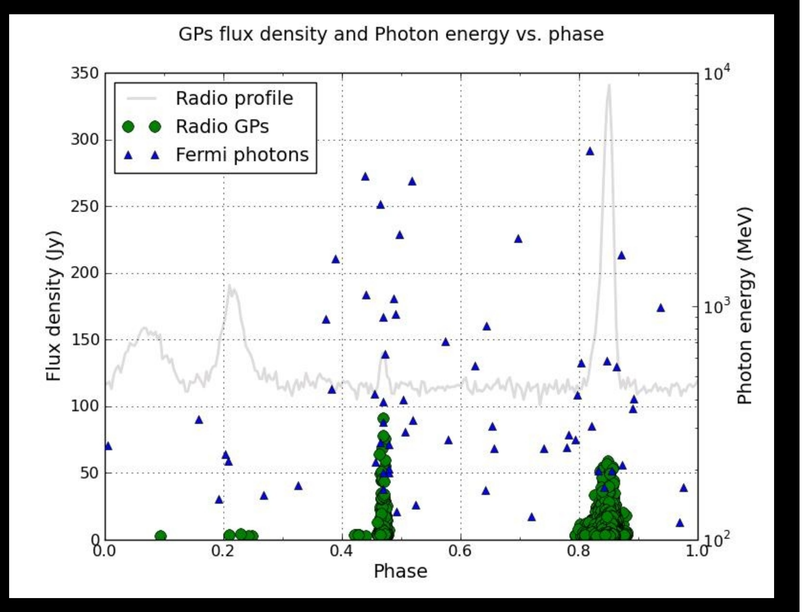

Figure 2. Flux density of GPs and Fermi photons vs. the phase of their occurrence within the Crab period. The radio profile from one of the GBT sessions is shown in the background (gray). Most of GPs occurred at the phases of the MP and IP, though several pulses, either giant pulses or regular single pulses, were detected at the phases of HFCs and even MP precursor.

Fermi data & correlation

For each observing radio session we extracted LAT data: diffuse class of events, energy-dependent ROI: θ < Max(1.6 – 3log(E/1000 MeV),1.3) deg (Grondin et. al). Total number of photons per 8 hours of simultaneous observations is 70 above 100 MeV and 11 above 1 GeV. Photons were barycentered with TEMPO2 using the same ephemeris as for radio GPs.

For every photon we searched for a GP within either 1 or 10 pulsar periods (33 and 330 ms). Since the rate of GPs varies significantly from session to session (due to scintillations), the search was performed for each day separately.

The mean number of spurious matches (i.e. when there is no true correlation) was assessed as the mean of binomial distribution with number of trials N = T_obs/(correlation window) and probability of success p = (n_GPs/N)*(n_gamma/N). However, this is quite a rough estimate since it does not take into account that GPs come in bursts (see Figure 4). Also, we didn't make any estimations yet about background gamma-flux which is especially essential at energies ~100 MeV.

Day (in Sep 2009)	Time of simultaneous observations (s)	Number of Giant Pulses	Photons with E >100 MeV					Photons with E >1 GeV				
			Number of photons	# of matches within **1** Crab period	mean expected # of accidental matches	# of matches within **10** Crab periods	mean expected # of accidental matches	Number of photons	# of matches within **1** Crab period	mean expected # of accidental matches	# of matches within **10** Crab periods	mean expected # of accidental matches
12	1551	4	7	0	0.0	0	0	1	0	0.0	0	0.0
14	3304	4166	11	2	0.5	8	4.6	2	2	0.1	2	0.8
19	3077	4096	7	1	0.3	4	3.1	2	0	0.1	1	0.9
20	1779	1069	2	0	0.0	0	0.4	1	0	0.0	0	0.2
21	1801	154	2	0	0.0	0	0.1	1	0	0.0	0	0.0
22	3871	1567	6	0	0.1	0	0.8	1	0	0.0	0	0.1
23	4710	9764	10	2	0.7	7	6.8	0				
24	1260	264	1	1	0.0	1	0.1	0				
25	7446	18299	19	2	1.5	10	15.4	3	0	0.2	2	2.4
28	2795	65	5	0	0.0	1	0	0				
Total	**31594**	**39448**	**70**					**11**				

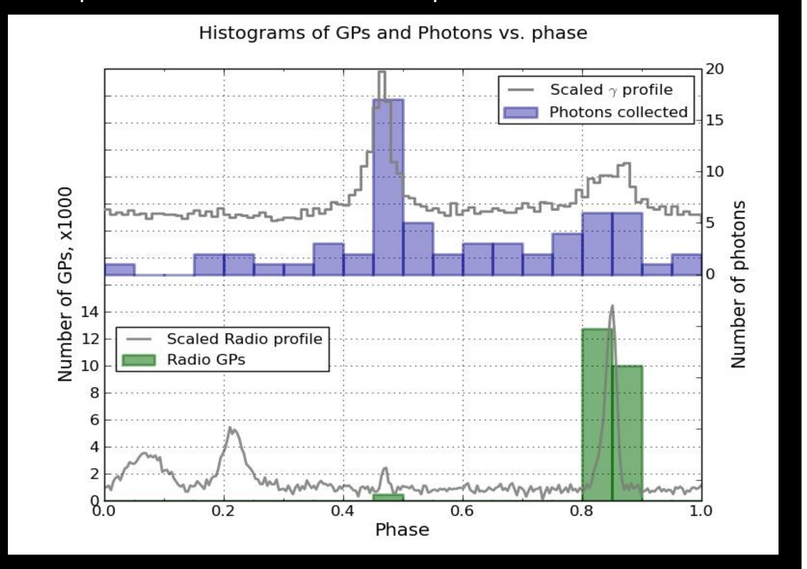

Figure 3. Histograms of GPs and Fermi photons during the simultaneous time. For illustrative purposes radio and γ scaled profiles are shown (gray). Scaled radio profile is from GBT session on Sep 25, 2009, and γ-profile is Fermi profile accumulated during Sep, 2009. Two profile components corresponding to MP and IP are clearly seen in both profiles. In agreement with Hankins & Eilek (2008) radio GPs occur more frequently at the phases of IP, while GPs in MP are stronger (see also Figure 2). Due to small photons sample, no definitive conclusion can be put forward, whether there is an average increase in counts rate in Fermi profile during the events of radio GPs.

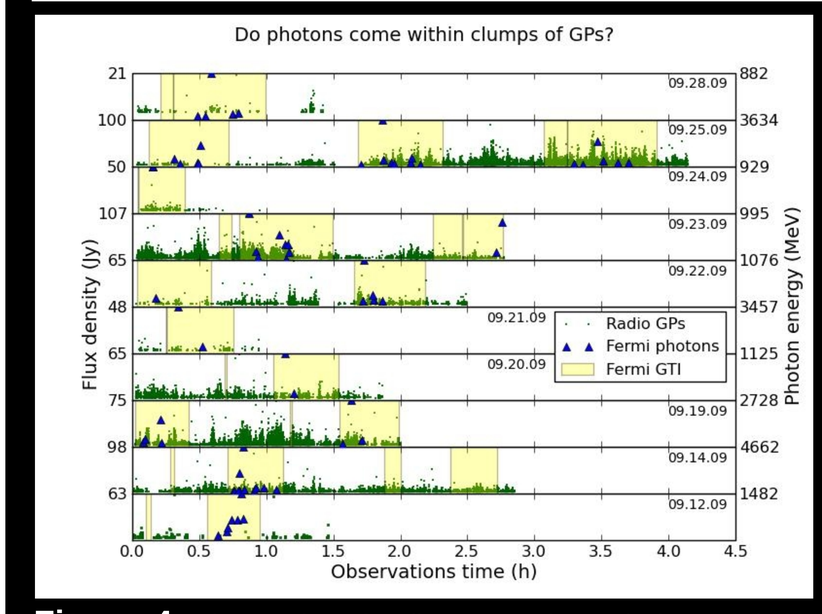

Figure 4. Time series of radio GPs and Fermi photons during 10 observing sessions. The values on Y-axes shows either the maximum flux density in radio (left) or the maximum photon energy (right) in the corresponding subplot. At high radio frequency of 8.9 GHz GPs occur in bursts or clumps due to scintillations with a characteristic scintillation time of about 10-20 min. However, scintillations can mask the intrinsic flux variability inherent to the pulsar. Apparently photons do also have a tendency to occur in clumps, and in some cases during the increase of the flux in radio. The latter does require a proper analysis though.

Summary

No obvious correlation was found between Fermi photons of energies > 100 MeV and radio giant pulses at the frequency of 8.9 GHz.

Current preliminary results indicate that fraction of photons closely accompanying high-frequency GPs is certainly less than 10% (N_matches/N_gamma, see the Table). In order to estimate this value more precisely, one needs to continue simultaneous observations, accumulating more photons and registering more GPs. Such campaign of Fermi / radio observations using 140-ft telescope at Green Bank Observatory (WV) and 42-ft telescope at Jodrell Bank Observatory at low frequencies is ongoing now. Non-correlation, if indeed true, may favor for coherence change as a reason for GP emission rather than variations in pair creation rate in the pulsar magnetosphere, or changes in beaming direction. In particular, the model of Lyutikov (2007) predicts correlation between high-energy photons and radio GPs at frequencies 4-10 GHz. Again, if radio and gamma-rays are indeed not correlated, then model either has to be tweaked, or such correlation exists only for VHE photons >~ 100 GeV. At this energy range Fermi, though sensitive, can not provide extensive sample of photons in reasonable time for correlation. At these energies Cherenkov detectors are much more promising.

Simple identification of time of arrivals of photons shows that they also come in groups similarly to radio GPs. Though in case of GPs this is caused by scintillations, they could potentially mask the flux variability intrinsic to the Crab pulsar as well. Then, we would expect groups of photons to concentrate with fraction of stronger GPs. And in fact, we do see the tendency of some groups of photons to cluster around strong GPs.

Using the current dataset, we are planning to do a more thorough analysis of TOA correlation between individual photons and radio GPs. There could be a time delay between time of arrival of Fermi photon and corresponding GP due to, for instance, different travel paths in the pulsar magnetosphere, or non-simultaneity in emitting radio and gamma-ray. We will introduce the delay between photon and GP time series and run the correlation analysis for many such trials. Also, gamma-photons may accompany only the brightest GPs or the clump of giant pulses as a whole. Obviously, a more detailed inquiry is required.

The National Radio Astronomy Observatory is a facility of the National Science Foundation operated under cooperative agreement by Associated Universities, Inc.